IEEE Access
Multidisciplinary | Rapid Review | Open Access Journal

Received November 28, 2018, accepted December 18, 2018, date of publication January 21, 2019, date of current version February 8, 2019.

Digital Object Identifier 10.1109/ACCESS.2019.2893941

A Wideband Dual-Polarized Omnidirectional Antenna for 5G/WLAN

LEI ZHAO[1,2], (Senior Member, IEEE), ZHAO-MIN CHEN[2], (Student Member, IEEE), AND JUN WANG[3]

[1]School of Information and Control Engineering, China University of Mining and Technology, Xuzhou 221116, China
[2]Jiangsu Key Laboratory of Education Big Data Science and Engineering, School of Mathematics and Statistics, Jiangsu Normal University, Xuzhou 221116, China
[3]State Key Laboratory of Millimeter-Waves, School of Information Science and Engineering, Southeast University, Nanjing 211189, China

Corresponding author: Lei Zhao (leizhao@jsnu.edu.cn)

This work was supported in part by the National Science Foundation of China under Grant 61771226, Grant 61372057, and Grant 61671223, in part by the Natural Science Foundation of the Jiangsu Higher Education Institutions of China under Grant 18KJA110001, and in part by the Natural Science Foundation of the Xuzhou of China under Grant KC18003.

ABSTRACT A compact wideband dual-polarized omnidirectional antenna with good isolation for the fifth generation/wireless local area networks communication is presented in this paper. The dual-polarized characteristic of the proposed antenna is achieved by combining a vertical polarization (VP) monopole antenna and horizontal polarization (HP) cross bow-tie antenna, which is excited by a 50 Ω Sub-Miniature-A (SMA) connector and a broadband feeding network, respectively. The size of the proposed antenna is only $0.38\lambda \times 0.38\lambda \times 0.27\lambda$ (with λ being the wavelength of the lowest frequency). The simulated isolation of the proposed dual-polarized omnidirectional antenna is below −38dB in the bandwidth from 2.3 GHz to 3.7 GHz (about 46.7%, $|S_{11}| < -10$ dB), taking no account of the commercial RF-Balun and SMA connectors. Moreover, the measured isolation of the proposed antenna with a feeding network is about −20 dB. The gain variations at the center frequency in the horizontal plane are 1.6 dB for VP element and 2.4 dB for HP element. And the lowest peak realized gains of the proposed cross bow-tie shaped antenna and the monopole antenna are about 4 dB and 2 dB, respectively. A prototype of the proposed dual-polarized omnidirectional antenna was fabricated to verify the simulated results, and the measured results are in a good agreement with the simulated ones.

INDEX TERMS Cross bow-tie, dual-polarized omnidirectional antenna, monopole, WLAN, 5G.

I. INTRODUCTION

The fifth generation (5G) wireless communication systems attract ours eyes on the deployment of commercial 5G systems, especially sub-6 GHz (around 3.5/4.5 GHz) band [1]–[3]. The 3.4 GHz to 3.6 GHz range was identified for International Mobile Telecommunication (IMT) at the World Radio-Communication Conference (WRC-15), and this spectrum is available globally, while the availability of the other parts of 3.3 GHz to 4.2 GHz varies for different regions and countries [4]. The 5G technology brings opportunities to development in the big Earth Village for the researchers and companies that are engaged in the study, and with many challenges. For modern 5G wireless communication systems, a compact wideband dual-polarized omnidirectional antenna and good isolation is indispensable.

Over the past decades, a series of dual-polarized antennas have been studied and designed [5]–[14], [16]–[19]. The feeding techniques are commonly used for dual-polarized antennas. Generally, the feeding probes, coupling slots and modified direct feeding structure [5]–[7] are usually employed in the feeding techniques. Moreover, the combination of vertical polarization (VP) antenna and horizontal polarization (HP) antenna [9]–[13], [16]–[19] is also an effective method to achieve dual-polarization. By integrating three polygonal radiation patches and three wideband slot loop structures, the design in [11] could operate from 1650 MHz to 2900 MHz for HP, and from 780 MHz to 2700 MHz for VP, respectively. And the gain variations are 3 dB for VP element and 2.5 dB for HP element. In [13], a wideband dual polarized antenna for spectrum monitoring systems from 190 MHz to 850 MHz was proposed, but the gain variations of the antenna need to be improved to meet the further requirement of applications. In order to improve the impedance matching and gain variations,

a design composing interconnected cross bow-tie antenna for HP was proposed [16]. However, the impedance bandwidth of the antenna may need to be broadened for serving in 5G communication systems and the isolation between ports need to be improved for the communication systems.

In this paper, a wideband dual-polarized omnidirectional antenna with good isolation based on the one in [16] is proposed for 5G/WLAN communication systems. The antenna achieves a compact structure by integrating an inverted-cone monopole antenna for VP and a cross bow-tie antenna for HP by using a small circular ground, which located in the middle of the cross bow-tie shaped antenna. In order to ameliorate the impedance matching and the omnidirectional radiation pattern of the HP cross bow-tie antenna, a semi-oval petal is designed to be a part of the arms of each bow-tie. Compared to the design in [16], the proposed antenna in this paper would have the following enhancements:

1) The omnidirectional operating frequency band covers 2.3 GHz-3.7 GHz, which can be used in the 2.4 GHz WLAN and 5G communication systems,
2) The isolation of proposed dual-polarized omnidirectional antenna can be below −38 dB across the operating band without taking the influence of RF-Balun and SMA connectors into consideration, and the measured isolation of the proposed antenna with the feeding network is about −20 dB across the operating band.
3) The lowest peak realized gain of the proposed cross bow-tie shaped antenna and the monopole antenna are about 4 dB and 2 dB, respectively.

II. ANTENNA GEOMETRY AND DESIGN

A. ANTENNA GEOMETRY

The geometry of the proposed wideband dual-polarized omnidirectional antenna is depicted in Fig. 1. The design combines a monopole antenna with a cross bow-tie antenna. Fig. 1(a) illustrates the whole configuration of the proposed antenna and the structure of feeding line with symmetry. The inverted-cone monopole antenna and the proposed antenna's substrates are shown in the Fig. 1(b).

For the VP element, it consists of an inverted-cone tube with a small circular ground integrated into the middle of the substrates and a cross bow-tie shaped antenna. It should be mentioned that the small circular ground and cross bow-tie shaped antenna act as the ground plane for VP antenna simultaneously. Moreover, the HP element is made up of a cross bow-tie shaped antenna (for this case, as a radiator), which each bow-tie arm consists of semi-oval petal, as shown in Fig. 1(c). Furthermore, a conductor ring with four corners are added in the cross bow-tie shaped antenna to ameliorate the impedance matching, and the symmetric feeding lines printed on the Rogers 4350B substrates are employed to improve the isolation of ports 2 and 3.

As shown in Fig.1, the dimension of the cross bow-tie shaped antenna are determined by the L_2, L_3, W, and W_5. L, L_1, denotes the size of conductor ring with four corners located around the cross bow-tie shaped antenna.

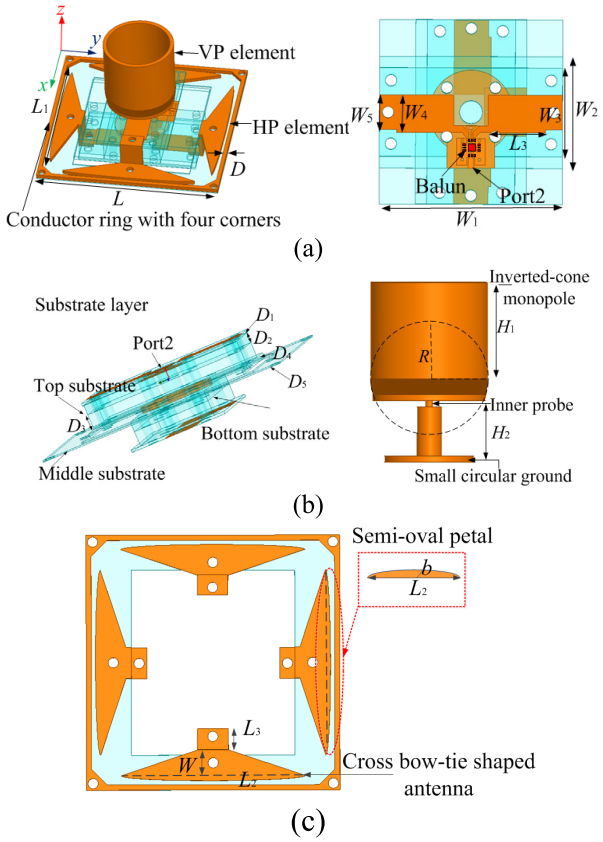

FIGURE 1. (a) The whole configuration of the proposed wideband omnidirectional antenna, the feeding structure of the proposed bow-tie shaped antenna, where only the feeding structure of the port 2 is shown since the symmetry of ports 2 and 3; (b) The structure of the proposed antenna's substrates and the geometry of the inverted-cone monopole antenna; (c) The proposed bow-tie shaped HP element surrounded by conductor ring with four corners.

The dimensions of substrate and feeding line are determined by the W_1, W_2, W_3, W_4, W_5, L_3, L_4, respectively. The thicknesses of the Rogers 4350B substrates are denoted by D_1, D_5. The thicknesses of the FR4 substrates are denoted by D_2, D_3, *and* D_4. And we have $L = 41.4$mm, $L_2 = 36$mm, $L_3 = 4$mm, $L_4 = 10$mm, $H = 28.2$mm, $H_1 = 15.6$mm, $H_2 = 9$mm, $R = 9.58$mm, $b = 1$mm, $W = 5$mm, $W_1 = 32$mm, $W_2 = 19.4$mm, $W_3 = 15.4$mm, $W_4 = 6.5$mm, $W_5 = 6$mm, $D_1 = 0.508$mm, $D_2 = 2$mm, $D_3 = 3$mm, $D_4 = 1$mm, $D_5 = 0.254$mm.

B. ANTENNA DESIGN

In order to obtain a dual-polarized omnidirectional antenna, the proposed antenna consists of a VP element and a HP element. The inverted-cone monopole antenna acts as a VP element. Compared with the concerning design in [16], this proposed design extends the radius and reduces the height to achieve a wider bandwidth and compact size. The outward travelling waves generated by its feed produce a vertically polarized radiation in the horizontal plane. In addition, the cross bow-tie shaped antenna surrounded by a conductor ring is designed to generate an omnidirectional HP radiation wave. The HP element is fed by a broadband feeding system

with a 90° phase difference and the same amplitude. In order to compact the dimension of the proposed antenna, a modified cross bow-tie acts not only as a HP element but also as a part of ground of VP element by using the small circular ground located in the middle of the substrates. And when the VP element is excited and HP element (ports 2 and 3) is connected to a matching load, the currents flow from the small ground to the cross bow-tie shaped arms, which excite the ground current distributions of the typical monopole antenna on cross bow-tie arms, which greatly compact the structure of the proposed antenna.

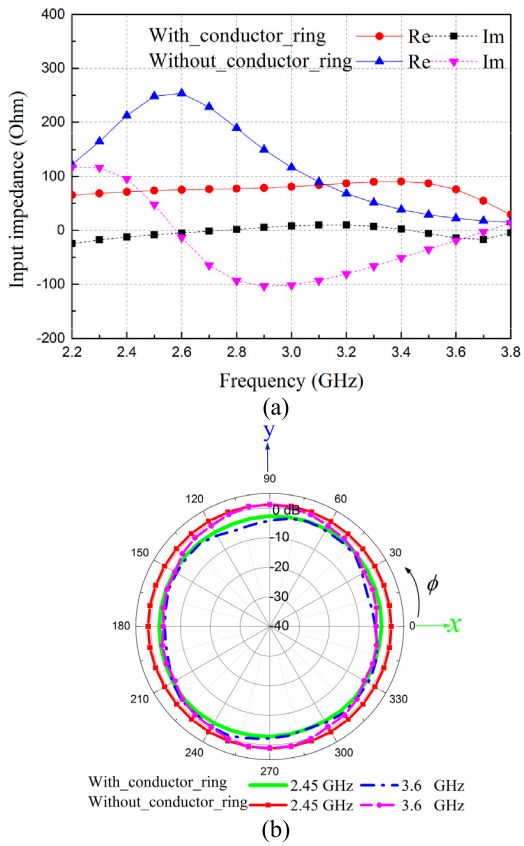

FIGURE 2. Simulated input impedance of port 2 and radiation pattern of the HP element in the horizontal plane with and without the conductor ring with four corners. (a) Input impedance of port 2. (b) Radiation pattern of the HP element.

The conductor ring with four corners around the bow-tie shaped antenna plays the important roles in two aspects: one is to improve the impedance matching; the other is to enhance gain variation of the omnidirectional radiation pattern. Since the symmetry of ports 2 and 3, only the input impedance of port 2 with and without conductor ring with four corners is depicted in Fig. 2(a). The inductive components of the conductor ring with four corners can compensate the capacitive components caused by the cross bow-tie dipole to improve the input impedance matching. As the impedance ratio (secondary/primary) of commercial RF-Balun (MTX2-73) used in the proposed antenna is two. In order to normalize the primary impedance to 50 Ω, the designed conductor ring with four corners is proposed to make the impedance (secondary) matching close to 100 Ω, which is beneficial to the design and fabrication of the proposed antenna with commercial RF-Balun. Furthermore, Fig. 2(b) illustrates that the conductor ring with four corners can enhance the gain variation of omnidirectional radiation pattern in the horizontal plane. The gain variations are reduced from 2.9 to 2.6 dB at 2.45 GHz and from 5.5 to 4.8 dB at 3.6 GHz.

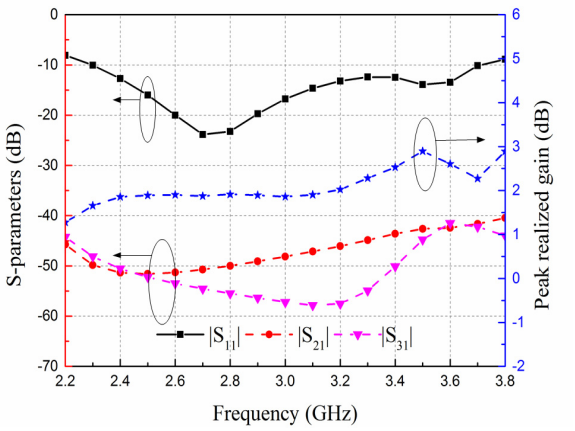

FIGURE 3. Simulated $|S_{11}|$ and gain values of the proposed inverted-cone monopole and the mutual coupling between the VP and HP elements.

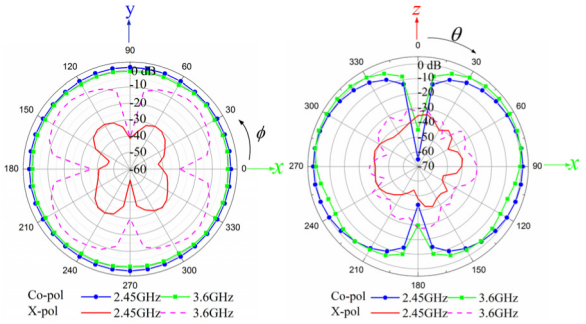

FIGURE 4. Simulated radiation patterns of the VP element at 2.45 and 3.6 GHz.

C. ANTENNA PERFORMANCE

The proposed antenna is designed and simulated according to the geometry of antenna and design principle discussed above using the ANSYS. As commercial RF -Baluns cannot be simulated in the ANSYS, the RF- Baluns need to be assumed as ideal devices and 50 Ω lumped ports with the same amplitude and a 90° phase difference are used for the HP element excitation. Fig. 3 illustrates the simulated reflection coefficient $|S_{11}|$ and gain values of the proposed VP element. As shown in Fig. 3, the VP element obtains a good impedance matching within a wide frequency range and the impedance bandwidths of $|S_{11}| < -10$dB is 1.4 GHz (from 2.3 GHz to 3.7 GHz, about 46.7%), and the lowest peak realized gain of the proposed VP element is about 2 dB in the operating bandwidth. The simulated radiation patterns of the VP element at 2.45 and 3.6 GHz are depicted in Fig. 4, which show that the gain variations of the VP element in the

horizontal plane are 0.8 and 1.2 dB at 2.45 and 3.6 GHz, respectively.

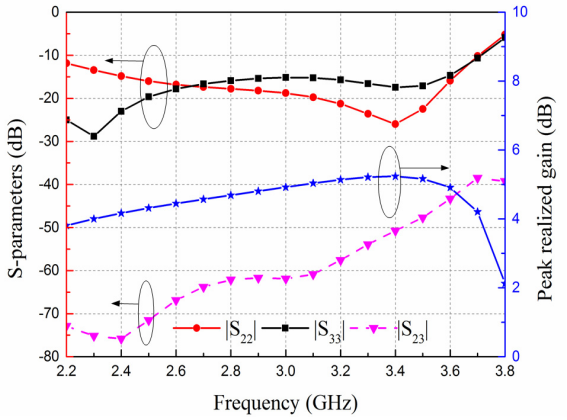

FIGURE 5. Simulated $|S_{22}|$, $|S_{33}|$ and gain values, isolation of two ports of HP element.

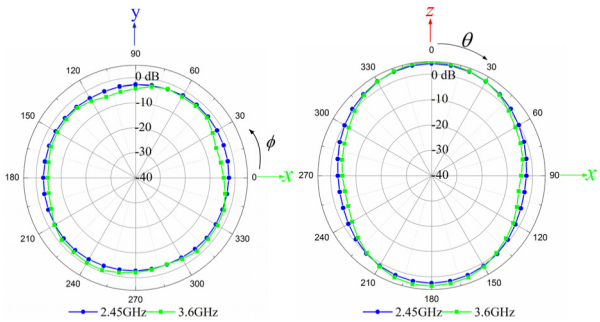

FIGURE 6. Simulated radiation patterns of the HP element at 2.45 and 3.6 GHz with the excitations of the same amplitude and a 90° phase deviation.

When the cross bow-tie shaped antenna (HP element) is excited with the same amplitude and a 90° phase difference, the simulation S-parameter results and omnidirectional radiation in the horizontal plane can be achieved and shown in Figs. 5 and 6, respectively. It is obvious to know the operating frequency (10 dB return loss) of the cross bow-tie shaped antenna is from 2.2 GHz to 3.7 GHz for $|S_{22}|$ and $|S_{33}|$, and the lowest peak realized gain of the proposed HP element is about 4 dB within the operating bandwidth. Fig. 6 displays the radiation patterns at 2.45 and 3.6 GHz, showing a good omnidirectional radiation patterns are obtained in the horizontal plane.

D. PARAMETER ANALYSIS

Since the cross bow-tie shaped antenna is fed by a 90° phase difference feeding network to radiate a horizontally polarized omnidirectional pattern by rotating the electric field, the phase information plays a vital role on the omnidirectional radiation pattern of the HP element. A parametric study on phase information is implemented to analyze the influnces on the radiation performance which is usefull for the practical design of a cross bow-tie shaped antenna. The simulated omnidirectional patterns of the HP element under excitations with different phase deviations (from 80° to 100°, step 5°) at 2.45 and 3.6 GHz in the horizontal plane are displayed in the Fig. 7. According to the Fig. 7(a), the gain variations are 1.5, 0.8, 2.2 dB at 2.45 GHz under the excitation of 80°, 90°, and 100° phase deviation, and the gain variations are 5.7, 4.8, 5.8 dB at 3.6 GHz under the excitation of 80°, 90°, and 100° phase deviation, as shown in Fig. 7(b), respectively.

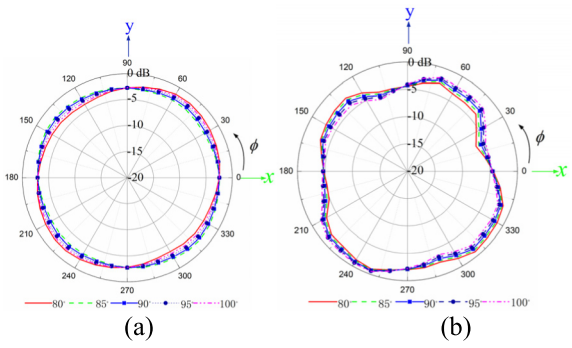

FIGURE 7. Simulated omnidirectional radiation patterns of the HP element under different excitations at 2.45 and 3.6 GHz in the horizontal plane. (a) 2.45 GHz. (b) 3.6 GHz.

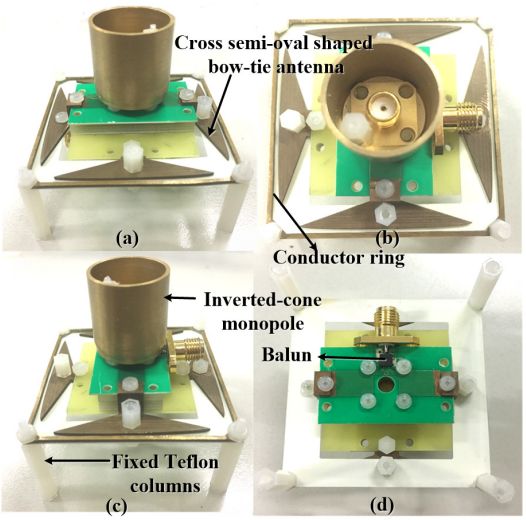

FIGURE 8. Photographs of the proposed antenna. (a) 3D view. (b) Top view. (c) Side view. (d) Bottom view.

III. EXPERIMENTAL RESULTS AND DISCUSSION

In order to verify the proposed wideband dual-polarized omnidirectional antennna with good performance, a prototype of the proposed antenna is fabricated, shown in Fig. 8. A 50Ω SMA connector is soldered on the inverted-cone monopole and inner probe is embedded in the small circular ground. For feeding the cross bow-tie, two 50 Ω SMA connectors are soldered on the feeding striplines printed onto the Rogers 4350B substrates. Meanwhile, two commercial RF-Balun (MTX2-73) are soldered onto its top and bottom feeding striplines. The measured and simulated S-parameters of the VP and HP elements are shown in Fig. 9(a) and (b).

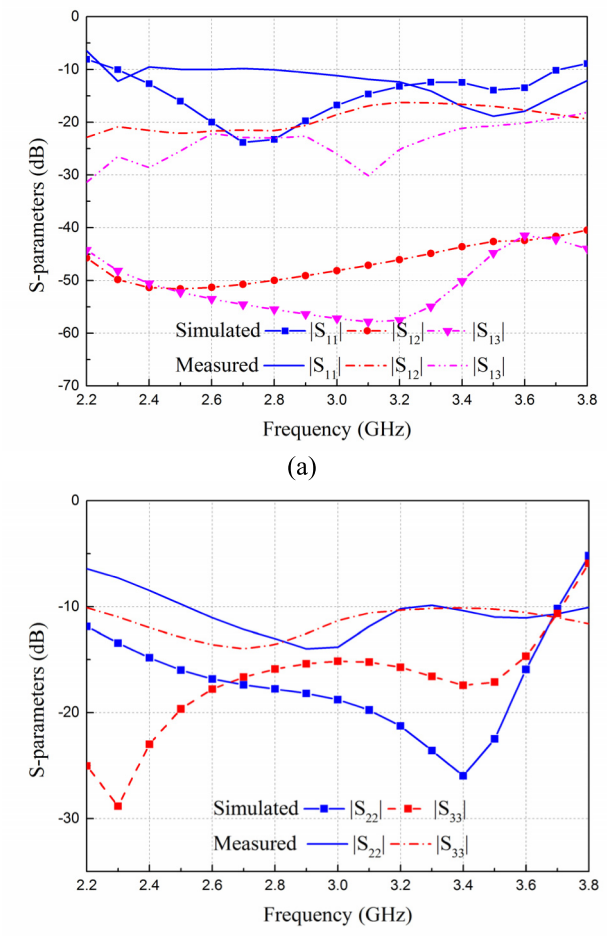

FIGURE 9. Simulation and measured results of the proposed antenna. (a) VP element and its mutual coupling with the HP element and (b) HP element.

When the VP element is excited, the simulated impedance bandwidth ($|S_{11}| < -10$dB) of the VP element is from 2.3 GHz to 3.7 GHz (46.7%) and from 2.25 GHz to 3.8 GHz (51.2%) for the measured one, respectively. Fig. 9(b) displays the impedance bandwidth of the HP element which is from 2.2 GHz to 3.7 GHz for $|S_{22}|$ and $|S_{33}|$, whereas the measured bandwidth is from 2.5 GHz to 3.8 GHz for $|S_{22}|$ and 2.2 GHz to 3.8 GHz for $|S_{33}|$ when the HP is excited.

In order to verify the proposed omnidirectional HP element experimentally, a broadband feeding network which consists of a power divider and a 90° phase shifter is utilized to integrate ports 2 and 3 to achieve a HP omnidirectional radiation pattern, which are in Fig. 10(a). The return loss of the power divider and phase shifter is about 10 dB and phase deviation of the phase shifter is within 5°. The measured results agree well with the simulated ones within the required band. The measured S-parameters of the proposed dual-polarized antenna with the feeding network is presented in the Fig. 10(b). It is obviously that the proposed antenna obtains a desired bandwidth (impedance bandwidth), which is from 2.2 GHz to 3.7 GHz for the VP element and 2.2 GHz

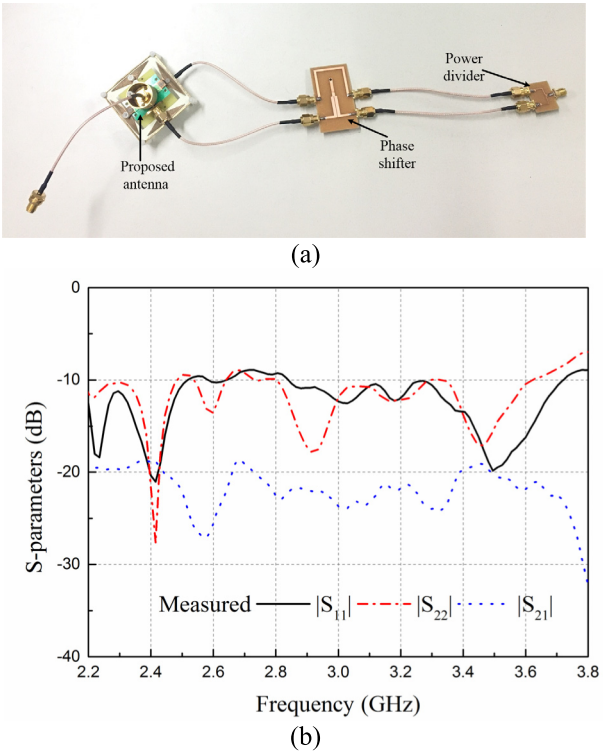

FIGURE 10. (a) Configuration of the proposed antenna with a broadband feeding network. (b) Measured S-parameters of the proposed antenna with a broadband feeding network.

TABLE 1. Performance comparison of existing dual-polarized omnidirectional antennas.

Ref.	Sizes (λ_L) (λ_L at the Lowest Frequency)	Type of polarization	Bandwidth (10-dB Return Loss)	Gain variation
[9]	0.57×0.43×0.43	VP HP	35% 30%	0.5 dB 1.5 dB
[10]	0.45×0.45×0.31	VP HP	17.4% 35%	<1.5 dB <1.5 dB
[16]	0.35×0.35×0.25	VP HP	47.6% 41.5%	0.7 dB 2.3 dB
This work	0.38×0.38×0.27	VP HP	46.7% 50.8%	1.6 dB 2.4 dB

to 3.6 GHz for the HP element. The measured S-parameters of the VP and HP element are a little beyond −10 dB, which is caused by the SMA connectors and the commercial RF-Balun. Additionally, the isolation between the VP and HP ports keeps about −20 dB. In addition, Fig. 11(a) shows the measurement environment of the proposed antenna. The measured and simulated radiation patterns of the proposed antenna are presented in Fig. 11(b) and (c), which show a good omnidirectional radiattion patterns for VP and HP.

Since the standard circularly polarized horn antenna was unavailable for the measurement system used, radiation pattern of the HP element were not measured directly. The radiation pattern is synthesized by measuring two linear polarization components of the HP element with the

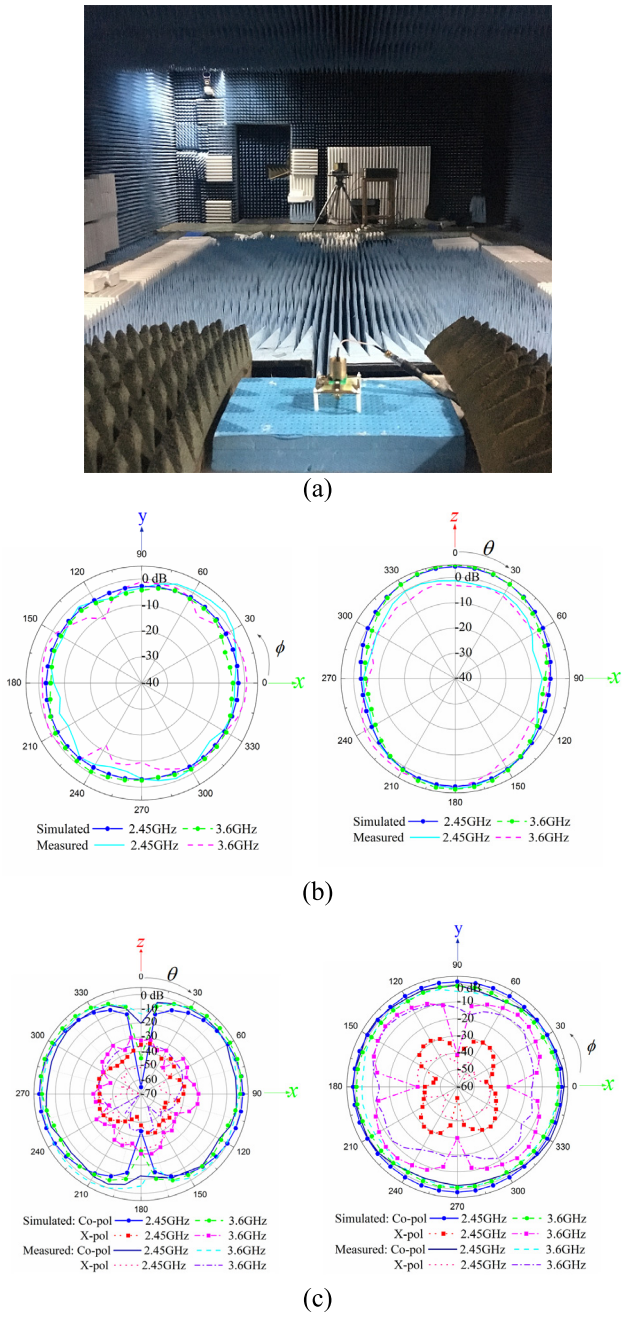

FIGURE 11. **(a) Measured environm of the proposed antenna and simulated *and measured radiation patterns of (b) HP element and (c) VP element.***

postulation of a 90° phase deviation for the two ports. Therefore, the effects of the conductor ring with four corners could not be taking into account in the synthesized radiation pattern. Table 1 summarizes the performance comparison of existing dual-polarized omnidirectional antennas. Compared to other dual-polarized omnidirectional antennas, our proposed antenna exhibits the advantages in return-loss bandwidth. And the antenna size, gain variation also have a good performance.

IV. CONCLUSION

A wideband dual-polarized omnidirectional antenna with good isolation was presented for 5G/WLAN applications. For enhancing the impedance matching, the semi-oval petals are designed and optimized for the crossed bow-tie antenna. Combining a monopole antenna for VP and a cross bow-tie shaped antenna with the symmetric feeding structure for HP, the proposed antenna obtains good isolation. The measured results perform good agreement with the simulated ones, which illustrates that the proposed dual-polarized omnidirectional antenna has achieved a good isolation, a wide bandwidth.

REFERENCES

[1] S. Saxena, B. K. Kanaujia, S. Dwari, S. Kumar, and R. Tiwari, "MIMO antenna with built-in circular shaped isolator for sub-6 GHz 5G applications," *Electron. Lett.*, vol. 54, no. 8, pp. 478–480, Apr. 2018.

[2] R. Wu and Q.-X. Chu, "Multi-mode broadband antenna for 2G/3G/LTE/5G wireless communication," *Electron. Lett.*, vol. 54, no. 10, pp. 614–616, May 2018.

[3] M. Jaber, M. A. Imran, R. Tafazolli, and A. Tukmanov, "5G backhaul challenges and emerging research directions: A survey," *IEEE Access*, vol. 4, pp. 1743–1766, Apr. 2016.

[4] J. Lee, "Spectrum for 5G: Global status, challenges, and enabling technologies," *IEEE Commun. Mag.*, vol. 56, no. 3, pp. 12–18, Mar. 2018.

[5] C. Wu, C. Lu, and W. Cao, "Wideband dual-polarization slot antenna with high isolation by using microstrip line balun feed," *IEEE Antennas Wireless Propag. Lett.*, vol. 16, pp. 1759–1762, 2017.

[6] R. Lian, Z. Wang, Y. Yin, J. Wu, and X. Song, "Design of a low-profile dual-polarized stepped slot antenna array for base station," *IEEE Antennas Wireless Propag. Lett.*, vol. 15, pp. 362–365, 2016.

[7] Y. Liu, X. Li, L. Yang, and Y. Liu, "A dual-polarized dual-band antenna with omni-directional radiation patterns," *IEEE Trans. Antennas Propag*, vol. 65, no. 8, pp. 4259–4262, Aug. 2017.

[8] A. Alieldin *et al.*, "A triple-band dual-polarized indoor base station antenna for 2G, 3G, 4G and Sub-6 GHz 5G applications," *IEEE Access*, vol. 6, pp. 49209–49216, 2018.

[9] Y. Fan, X. Liu, B. Liu, and R. Li, "A broadband dual-polarized omnidirectional antenna based on orthogonal dipoles," *IEEE Antennas Wireless Propag. Lett.*, vol. 15, pp. 1257–1260, 2016.

[10] X.-W. Dai, Z.-Y. Wang, C.-H. Liang, X. Chen, and L.-T. Wang, "Multiband and dual-polarized omnidirectional antenna for 2G/3G/LTE application," *IEEE Antennas Wireless Propag. Lett.*, vol. 12, pp. 1492–1495, 2013.

[11] X. Quan and R. Li, "A broadband dual-polarized omnidirectional antenna for base stations," *IEEE Trans. Antennas Propag.*, vol. 61, no. 2, pp. 943–947, Feb. 2013.

[12] B. Li, Y.-Z. Yin, W. Hu, Y. Ding, and Y. Zhao, "Wideband dual-polarized patch antenna with low cross polarization and high isolation," *IEEE Antennas Wireless Propag. Lett.*, vol. 11, pp. 427–430, 2012.

[13] J. Wang, Z. Shen, and L. Zhao, "Wideband dual-polarized antenna for spectrum monitoring systems," *IEEE Antennas Wireless Propag. Lett.*, vol. 16, pp. 2236–2239, 2017.

[14] Z. Zhao, J. Lai, B. Feng, and C.-Y.-D. Sim, "A dual-polarized dual-band antenna with high gain for 2G/3G/LTE indoor communications," *IEEE Access.*, vol. 4, pp. 61623–61632, 2016.

[15] H. Wen, Y. Qi, Z. Weng, F. Li, and J. Fan, "A multiband dual-polarized omnidirectional antenna for 2G/3G/LTE applications," *IEEE Antennas Wireless Propag. Lett.*, vol. 17, no. 2, pp. 180–183, Feb. 2018.

[16] J. Wang, L. Zhao, Z.-C. Hao, and J.-M. Jin, "A wideband dual-polarized omnidirectional antenna for base station/WLAN," *IEEE Trans. Antennas Propag.*, vol. 66, no. 1, pp. 81–87, Jan. 2018.

[17] H. Huang, Y. Liu, and S. Gong, "Broadband dual-polarized omnidirectional antenna for 2G/3G/LTE/WiFi applications," *IEEE Antennas Wireless Propag. Lett.*, vol. 15, pp. 576–579, 2016.

[18] D. Guo, K. He, Y. Zhang, and M. Song, "A multiband dual-polarized omnidirectional antenna for indoor wireless communication systems," *IEEE Antennas Wireless Propag. Lett.*, vol. 16, pp. 290–293, 2017.
[19] Y. Liu, J. Xue, H. Wang, and S. Gong, "Low-profile omnidirectional dual-polarised antenna for 2.4 GHz WLAN applications," *Electron. Lett.*, vol. 50, no. 14, pp. 975–976, Jul. 2014.

LEI ZHAO (M'09–SM'18) received the B.S. degree in mathematics from Jiangsu Normal University, China, in 1997, the M.S. degree in computational mathematics, and the Ph.D. degree in electromagnetic fields and microwave technology from Southeast University, Nanjing, China, in 2004 and 2007, respectively.

He joined Jiangsu Normal University, Xuzhou, China, in 2009, where he is currently a Professor, and also the Director of the Center for Computational Science and Engineering. From 2007 to 2009, he was with the Department of Electronic Engineering, The Chinese University of Hong Kong, as a Research Associate. In 2011, he was with the Department of Electrical and Computer Engineering, National University of Singapore, as a Research Fellow. From 2016 to 2017, he was with the Department of Electrical and Computer Engineering, University of Illinois at Urbana-Champaign, Urbana, IL, USA, as a Visiting Scholar. He has authored and co-authored over 50 referred journal and conference papers. His current research interests include antennas design and its applications, computational electromagnetics, electromagnetic radiation to human's body, and spoof surface plasmon polaritons design and its applications. He serves as an Associate Editor for the IEEE Access, an Associate Editor-in-Chief for the *ACES Journal*, and a Reviewer for multiple journals and conferences, including the IEEE Transactions on Antennas and Propagation, the IEEE Access, the IEEE Antennas and Wireless Propagation Letters, *Progress in Electromagnetics Research*, the *ACES Journal*, and other primary electromagnetics and microwave related journals.

Dr. Zhao was the TPC Chair of the 2018 Cross Strait Quad-Regional Radio Science and Wireless Technology Conference. He has been an elected TPC member of the IEEE MTT-S International Microwave Workshop Series on RF and Wireless Technologies for Biomedical and Healthcare Applications, since 2013, a TPC member of the 2010 International Conference on Microwave and Millimeter Wave Technology, a TPC member of the 2012 International Conference on Microwave and Millimeter Wave Technology, a TPC member of the 2013 Cross Strait Quad-Regional Radio Wireless Conference, and a TPC member of the 2014 Cross Strait Quad-Regional Radio Wireless Conference.

ZHAO-MIN CHEN was born in Jiangsu, China. She received the B.S. degree from Jiangsu Normal University, Xuzhou, China, in 2016, where she is currently pursuing the M.S. degree. Her research interests include design of RF/ microwave antennas and filters.

JUN WANG was born in Jiangsu, China. He received the B.S. and M.S. degrees from Jiangsu Normal University, Xuzhou, China, in 2013 and 2017, respectively. He is currently pursuing the Ph.D. degree with Southeast University, Nanjing, China. His research interests include the design of RF/microwave antennas and phase shifter.